Gut Microbiome Alteration of Cold-adapated Antarctic copepod Tigriopus kingsejongensis with Temperature Changes and Developmental Stages

Han Na Oh
Chung-Ang University
Myeong Nu Ri
Chung-Ang University
Taeyune Kim
Chung-Ang University
Gi-Sik Min
Inha University
Sanghee Kim
Korea Polar Research Institute
Woo Jun Sul (sulwj@cau.ac.kr)
Chung Ang University - Anseong Campus

Research Article

Keywords: climate change, Antarctica, copepods, gut microbiome, virulence factors, chitinase

Posted Date: June 15th, 2021

DOI: https://doi.org/10.21203/rs.3.rs-611858/v1

Abstract

Tigriopus kingsejongensis, a copepod species, reported from the King Sejong Station, Antarctica, serves as a valuable food resource in ecosystems. Some copepods were temperature-sensitive in growth and post-embryonic development. We cultured *T. kingsejongensis* at three different temperatures (2°C, 8°C, and 15°C) in a laboratory to observe the alterations in the stool microbiome of copepods depending on the cultivation temperature and developmental stages. We observed copepod gut microbiome changes by increasing temperatures: a lower microbial diversity, a higher abundance of aquatic microbes, *Vibrio*, and a lower abundance of the psychrophilic microbes, *Colwellia*. Also, the copepod gut microbiome, according to the developmental stage, was changed: a lower microbial diversity in egg-attached copepods than nauplius at 8°C. We further analyzed three shotgun metagenomes from *T. kingsejongensis* stool samples at different temperatures and obtained 44 metagenome-assembled genomes (MAGs). We noted that MAGs of *V. splendidus* D contained glycosyl hydrolase (GHs) encoding chitinases and virulence factors with higher relative abundance at 15°C than at lower temperatures. These results that temperature and developmental stages affect the gut microbiome of copepods are helpful to understand the changes in the low-temperature adapted copepod with climate change.

Introduction

Copepods are small crustacean zooplankton mostly found in marine and freshwater habitats [1]. In the marine, copepods that may constitute up to 80 % of the mesozooplankton (Planktonic animals in size range 0.2–20 mm) biomass are known as symbiotic with aquatic animals and invertebrates [2, 3]. Copepods are key components of the aquatic food web as major consumers of primary producers, phytoplankton, and food for higher trophic levels, such as fish [4, 5]. These small copepods have an important role as prey for fish and other zooplanktivorous consumers, and so, the presence of copepods is an indicator of the naturally mature/stable ecosystem [6].

With increasing focus on microbiological investigations in copepods', many studies examine the copepods' gut microbiome. The copepods' gut, skin, oral region, anus, and egg case of females are known as the place where the attachment of bacterial cells occurs and to have their microbial communities [7, 8]. The microbiome of marine invertebrates and crustaceans has been reported to be associated with functions such as digestion, uptake of nutrients, reproduction, immune response, and other defenses in hosts [9–11]. According to Jean M. Harris, terrestrial vertebrates and invertebrates, and aquatic invertebrates show associations between the microbiome and the host [9]. Sachiko Nagasawa and Takahisa Nemoto noted the gut microbiome of metazoans, crustaceans, and animals [10]. Yeh et al. suggested that the gut microbiome of copepod is shaped by copepod feeding and the resident microbiome in the ocean and influences the metabolism and reproduction of other bacteria [12]. Moreover, they reported that the dominant bacteria Proteobacteria and Bacteroidetes presented at copepods' gut using 16S rRNA gene sequencing. Gerdts et al. revealed that Proteobacteria was the dominant phylum in the pellet in four frequently occurring copepod species using denaturing gradient gel electrophoresis (DGGE) and 16S rRNA gene sequencing [11]. Among the complex microbial community,

bacteria belonging to the Vibrionaceae family are commonly found in plankton [13]. Bacteria colonizing copepods' gut and body surfaces utilize chitin as the carbon and nitrogen sources and attract organic and inorganic nutrients and biomasses produced by copepods' fecal pellet and feeding [14]. For efficient chitin utilization, marine bacteria, including *Vibrio* species, require chitinase [15, 16]. The exoskeletons of copepods are composed of chitin, and bacterial chitinase may be involved in host pathogenesis and growth [17]. Besides, bacterial virulence factors are required to survive bacteria and are often involved in direct interactions with the host's defense mechanisms and growth. However, most studies have used cultivation-dependent approaches and molecular cloning methods and showed limited bacterial community structure and genes in copepods' bacterial colonization areas [18, 19].

In this study, we conduct the metagenome sequencing and bioinformatics analysis for examining copepods' gut microbiome. According to environmental and regional distribution, we intend to understand their role and function and observe gut microbial community composition changes and their genetic information by copepods' growing temperatures and development stages. The key objective is to see how cold-adapted Antarctic copepods and their gut microbiome change by experimentally applying temperature rise caused by global climate change.

Methods

Sample collection

Tigriopus kingsejongensis was isolated from tidal pools on the coast of the Barton Peninsula in Maxwell Bay (628140S, 588460W), King George Island, Antarctica [20]. Seawater collected with *T. kingsejongensis* from the same area in the tidal pool was used to cultivate and wash the copepods after filtration and sterilization. *T. kingsejongensis* was cultivated in a 2 l flask containing natural seawater (filtered using 0.2 μm filters) with moderate shaking at a 12:12 h light:dark cycle. The copepods were maintained at 8°C and 15°C before the experiment and were fed frozen *Chlorella* (purchased from Eleven Street Co.,Ltd). After 2–48 h of incubation, their stool was collected and used as samples for analyzing the stool microbial community. Seawater was used in the experiment after filtration and sterilization following the methods of Lee et al. [21]. Adult copepods were transferred to three different temperatures, namely 2°C, 8°C, and 15°C, after washing with sterilized seawater. To determine the temperature at which *T. kingsejongensis* can grow and propagate well, the standard temperature for artificial culture was set at 8°C, and copepods with eggs were selected to grow at this temperature. Nauplii hatched from the eggs of copepods were isolated. To compare the stool microbial community of different *Tigriopus* species, adult *T. japonicus* isolated from the tidal pool of Seonnyeo Rock Beach, Korea, was cultured at 15°C.

DNA extraction and 16S rRNA gene amplicon sequencing

DNA from the stool samples of copepods was extracted using pooled (n = approximately 100) 180–220 mg stool samples at each temperature and developmental stage using the QIAGEN QIAamp Fast DNA Stool Mini Kit. The concentration and purity of the extracted DNA were measured using a NanoDrop 2000 spectrophotometer (Thermo Fisher Scientific Inc., Waltham, MA, USA). For each stool sample, the V4-V5

region of the 16S rRNA gene was amplified by amplicon PCR using the barcoded fusion primers 518F-926R and Nextera XT Index II primer 2. In brief, the forward primer 5'-TCG TCG GCA GCG TCA GAT GTG TAT AAG AGA CAG CCA GCA GCY GCG GTA AN-3' contained the Illumina sequencing primer. The reverse primer 5'-GTC TCG TGG GCT CGG AGA TGT GTA TAA GAG ACA GCC GTC AAT TCN TTT RAG T-3' contained the Illumina pre-adapter. The amplification condition consisted of an initial denaturation at 95°C for 3 min; 25 cycles of amplification involving denaturation at 95°C for 30 s, annealing at 55°C for 30 s, and elongation at 72°C for 30 s; and a final extension at 72°C for 5 min. The amplified PCR products were purified using AMPure XP beads. Index PCR was performed under the same conditions as the amplification procedure, with the exception that eight amplification cycles were used. The obtained product was pooled for the Illumina Miseq sequencing library after quantification using PicoGreen and Nanodrop. The final product was quantified by qPCR according to the qPCR Quantification Protocol Guide (using KAPA Library Quantification Kits for Illumina sequencing platforms), and the quality was assessed using the LabChip GX HT DNA High Sensitivity Kit (PerkinElmer, Massachusetts, USA). Paired-end (2 × 300 bp) sequencing was performed by Macrogen using the MiSeq™ platform (Illumina, San Diego, USA).

Bacterial community analysis

The obtained sequences were processed using meren/illumina-utils [22] and the Quantitative Insights into Microbial Ecology (QIIME) pipeline (v.1.9.1) [23]. Paired-end sequence reads were merged with quality-based filtering using default parameters (the P-value was 0.3, Q-score was 10, and quality filter was Q30). Sequences that did not contain the primer sequence or contained an uncorrectable primer sequence were removed from the analysis. The merged sequences were clustered into operational taxonomic units (OTUs) with a sequence similarity threshold of 99% using the de novo UCLUST method [24]. Representative sequences of OTUs were used to identify the taxonomy using the Silva 132 reference database through the RDP classifier with a 0.5 minimum support threshold [25, 26]. Then, OTUs assigned to chloroplast and mitochondria were removed from our datasets. To assess the alpha diversity of the copepod's stool microbiome, the richness index (Chao1) was calculated using the QIIME script. Principal coordinate analysis (PCoA) was performed to evaluate the differences in the composition of microbial communities among the samples on the Bray–Curtis distance matrices.

Whole genome amplification (WGA) and metagenome sequencing

WGA was performed using the QIAGEN REPLI-g Mini Kit because of an insufficient quantity of DNA for metagenome sequencing. The stool samples of adult *T. kingsejongensis* at 2°C, 8°C, and 15°C were amplified. In total, 2.5 µl of the template DNA was added to a 1.5 ml microcentrifuge tube, following which 2.5 µl of the buffer D1 was added to the DNA. The DNA–buffer mixture was centrifuged and incubated at room temperature for 3 min. After the addition of 5 µl of the buffer N1, 40 µl of the master mix (10 µl of nuclease-free water, 29 µl of REPLI-g Mini Reaction Buffer, and 1 µl of REPLI-g Mini DNA Polymerase) was added to the sample and incubated at 30°C for 10–16 h. The sample was heated for 3 min at 65°C with REPLI-g Mini DNA Polymerase. Finally, the amplified DNA was quantified and qualified

using PicoGreen and agarose gel electrophoresis. To prepare the sequencing library, 100 ng of genomic DNA for a 350 bp insert size was fragmented using Covaris. The fragmented DNA was blunt-ended and phosphorylated. After end repair, the appropriate library size was selected using different ratios of sample purification beads. A single “A” was ligated to the 3' end, and Illumina adapters were ligated to the fragments. The final ligated product was quantified by qPCR according to the qPCR Quantification Protocol Guide, and the quality was assessed using the Agilent Technologies 2200 TapeStation (Agilent Technologies, Palo Alto CA, USA). The final samples were sequenced on the Illumina HiSeq™ 4000 platform (Illumina, San Diego, USA) as paired-end (2 × 100 bp) reads.

Metagenomic data analysis: Preprocessing and assembly

Shotgun metagenomic sequencing of the stool samples collected from adult *T. kingsejongensis* (after wash) at three different temperature conditions yielded 100,227,276 pair-end reads. Preprocessing of the metagenomic data was performed for the quality check and duplicate removal steps. The sequence quality was checked using FaQCs included in the Empowering the Development of Genomics Expertise (EDGE) pipeline, with a Q-score of 20 being the quality filter [27]. Duplicate reads were then removed using FastUniq with quality-filtered reads [28]. After the preprocessing steps, a total of 92,081,431 pair-end reads were used for metagenomic data analysis. Co-assembly of the metagenomic data was performed using MEGAHIT v1.1.3 with the option “--meta-sensitive presets.” Contigs less than 500 bp were discarded [29]. Finally, 112,246 contigs were generated with 325,730,737 bp, a maximum of 881,242 bases, and 9,035 N50 bases.

Metagenomic phylogenetic analysis: Taxonomic classification and genome reconstruction

CONCOCT, which uses a Gaussian mixture model and a dimension reduction algorithm with PCA based on the coverage, was used to reconstruct metagenome-assembled genomes (MAGs) from the metagenomic data [30]. To perform CONCOCT, original contigs longer than 20 kb were cut into fragmented contigs of 10 kb to enable more accurate coverage and reduce the impact of chimeric assemblies. Then, reads were mapped to fragmented contigs using BWA-MEM with default parameters [31]. CONCOCT was performed using fragmented coverage information with default parameters. Fragmented contigs were merged with the original contig, and a total of 138 genomes were reconstructed using a co-assembly contig.

Metagenomic data analysis: Pruning of MAGs

For genome quality, pruning of the genomes was performed employing Additional Clustering Refiner (ACR; https://github.com/hoonjeseong/acr). Overall, prediction of the open reading frame of contigs and annotation of single-copy proteins was performed using prodigal and HMMER, respectively. K-means clustering using scikit-learn v0.20.2 was performed based on the coverage of mapped reads. The 120 ubiquitous single-copy proteins were used for calculating completeness and redundancy of each MAG, for which we obtained more than MAG-Quality-score (Completeness-5×Redundancy) was 50. MAGs which were MAG-Quality-score < 50 were removed after the pruning step, and pruned MAGs are denoted

by '-' (e.g. Flavobacteriales_C.68.Bac to Flavobacteriales_C.68 − 0.Bac and Flavobacteriales_C.68 − 1.Bac). In the end, we obtained 44 high-MAG-Quality-score MAGs. For 44 pruned MAGs, we assigned taxonomy using Genome Taxonomy Database Toolkit (GTDB-Tk) [32].

Metagenomic data analysis: Carbohydrate-active enzymes (CAZymes) and virulence factors

The resulting genes in MAGs were predicted using Prodigal v2.6 included in the Prokka pipeline v1.13.3. CAZymes were annotated using run-dbcan v2.0.6 [33]. Three tools were used for detecting CAZomes: HMMER search, DIAMOND search, and Hotpop search. CAZymes detected in more than two tools were selected, yielding a total of 1,991 predicted CAZymes. To compare the genes found in MAGs from three *T. kingsejongensis* stool samples, the relative abundance of CAZymes was calculated as RPKM using featureCounts. Moreover, BLASTp was performed against the Virulence Factor Database (VFDB) to assess the virulence factors in these MAGs [34]. Only genes with ≥ 60% identity and ≥ 0.5 sequence coverage were considered associated with virulence factors and used for further analyses. To compare the distribution of virulence factors found at different cultivation temperatures, RPKM of virulence factors, such as CAZymes, was calculated.

Results

Characteristics of the copepod stool microbiome

To identify the differences in the stool microbiome of Antarctic copepods depending on temperatures, we collected the pooled (approximately 100 copepods) stool microbiome of *T. kingsejongensis* at three cultivation temperatures (2°C, 8°C, and 15°C; T.2, T.8, and T.15 groups, respectively) during different developmental stages (nauplii, egg-attached, and adult stages; the adult group was separated to before (BW) and after (AW) wash of seawater) (Fig. 1a). We observed that one-fifth to one-third of female egg sacs detached early and often failed to hatch when *T. kingsejongensis* was cultivated at 20°C. Through repeated experiments, we considered 15°C to be a significant boundary temperature for optimal growth. We thus set the cultivation temperatures at 2°C, 8°C, and 15°C. On the other hand, *T. japonicas* showed slow growth and reproductive retardation at 8°C.

We also analyzed a total of 13 samples, including *T. japonicas* as control using 16S rRNA gene sequencing, and generated a total of 1,405,607 reads. The 949,990 merged sequences were generated and clustered into 25,305 OTUs based on 99% sequence identity. PCoA with Bray–Curtis distance matrices revealed a clear separation among copepod microbiomes, especially on cultivation temperatures (Fig. 1b). The stool microbiome composition differed with the cultivation temperature and with the developmental status of copepods. Regarding the alpha diversity of the stool microbiome, an increase in the cultivation temperature decreased the Shannon diversity index (Fig. 1c). Moreover, the microbial richness of nauplii was higher than that of egg-attached copepods. When comparing two different copepod species, we found that the Shannon diversity index of *T. kingsejongensis* was lower than that of *T. japonicas*.

Taxonomic overview of the stool microbial communities of T. kingsejongensis

From the analyzing stool microbial composition of copepods, we obtained 32 bacterial phyla and three dominant phyla, Bacteroidetes, Proteobacteria, and Epsilonbacteraeota, in the stool microbiome of *T. kingsejongensis* (Fig. 2). The most dominant phylum was Bacteroidetes, with an average abundance of 49.37% ± 12.5%, followed by Proteobacteria (45.79% ± 11.69%) and Epsilonbacteraeota (4.12% ± 4.54%). Other phyla, such as Firmicutes, Patescibacteria, and Spirochaetes, were also detected; however, their abundance was very low (less than 0.2%). At the genus level, the bacterial composition differed depending on the cultivation temperature of copepods. *Colwellia* (17.14% ± 1.16%), *Arcobacter* (9.06% ± 0.75%), and *Pacificibacter* (7.72% ± 1.43%) were the dominant genera in the T.2 group, while uncultured Cryomorphaceae (28.00%), NS3a marine group (21.07%), and *Vibrio* (14.12%) were predominant in the T.8 group. Notably, *Vibrio* (42.74% ± 15.95%) was dominant in the T.15 group, followed by uncultured Cryomorphaceae (19.57% ± 5.79%) and *Pseudoalteromonas* (7.74% ± 0.27%). From the comparison for the most abundant genera at the same temperature and different developmental stages of *T. kingsejongensis*, we revealed that uncultured Saprospiraceae (19.85% ± 1.80%) and *Vibrio* (12.99% ± 12.76%) were abundant in the stool samples of nauplii. The genera *Algoriphagus* (37.51%) was dominant, and *Vibrio* (0.10%) was minor in egg-attached *T. kingsejongensis*.

Recovery of MAGs from copepod gut microbiome

To examine the relationship of the microbiome with slow copepod growth and the reduced population of egg-attached copepods at 15℃, metagenome sequencing was performed using three pooled samples (AW adult of T.2, T.8, and T.15 stools) obtained from *T. kingsejongensis*. The DNA extracted from the three stool samples was sequenced. A total of 92,081,431 paired-end reads were co-assembled using MEGAHIT. Following genomic binning by CONCOCT, 44 high-quality MAGs with MAG quality scores > 50 were obtained; after pruning (Fig. 3a), taxonomic assignment of each MAG was performed using GTDB.

The most abundant phylum was Bacteroidota, followed by Proteobacteria, Patescibacteria, Campylobacterota, and Verrucomicrobiota (Fig. 3b). Flavobacteriaceae was the most frequently assigned taxon at the family level in the *T. kingsejongensis* stool microbiome. Of the 44 MAGs, only three were assigned to the species level: *V. splendidus* D, *Croceibacter atlanticus*, and *Pseudomonas* E GCF_001050345.1. The most predominant MAGs were *Arcobacter*, 1G12 within the order Flavobacteriales, and *V. splendidus* D in the AW T.2, T.8, and T.15 groups, respectively. Interestingly, *V. splendidus* D, known as a dominant culturable *Vibrio* found in seawater, had a higher relative and absolute abundance in the AW T.15 group. In addition, MAGs were distributed in three samples; however, their abundance depended on the cultivation temperature. The abundances of MAGs belonging to Proteobacteria (*V. splendidus* D, *Loktanella*, and *Pseudoalteromonas*) and to Bacteroidota (*Maribacter*, *C. atlanticus*, and *Polaribacter*) were higher with an increase in temperature. In contrast, *Bizionia*, LS-SOB, and UBA8649, belonging to Bacteroidota, decreased with an increase in temperature. However, some MAGs were evenly distributed in all the samples regardless of the cultivation temperature; these included those belonging to *Maribacter*, *Winogradskyella*, and LS-SOB.

Features and distribution of virulence factor-related genes in MAGs from T. kingsejongensis stool samples

To identify the virulence factors in the *T. kingsejongensis* stool microbiome, 44 MAGs were identified based on VFDB using BLASTp. A total of 351 virulence factors were found in all MAGs, except for SW10 (Bin0) and UBA1006 (Bin99). Thirty-two kinds of virulence factor genes were identified. Most virulence factors were more frequently observed in the AW T.15 group than in the AW T.2 and T.8 groups (Fig. 4a). The salicylate biosynthesis protein PchB (*pchB*), sugar nucleotidyltransferase (*Cj1416c*), and dTDP-4-dehydrohamnose 3,5-epimerase (*rfbC*) were the top three virulence factors in the copepod stool microbiome. The relative abundances of nine genes, including dTDP-4-dehydrorhamnose 3,5-epimerase (*rfbC*), the type III secretion system inner membrane export apparatus protein AscS (*ascS*), the flagellar basal body rod modification protein FlgD (*flgD*), the alginate regulatory protein AlgQ (*algQ*), and urease accessory protein (*ureG*), were higher in high temperature. On the other hand, the relative abundance of only one gene was higher in low temperature: N – acetylglucosaminyltransferase involved in polysaccharide intercellular adhesin (PIA) synthesis (*icaA*).

Comparison of the number of virulence factors in each MAG and the size of the MAG revealed that most MAGs did not contain a high number of virulence factors (Fig. 4b). Of these, MAGs belonging to *V. splendidus* D (Bin95), GCF_001050345.1 (Bin82), *Pseudoalteromonas* (Bin136), *Colwellia* (Bin64_0), and *Amphritea* (Bin115) contained many virulence factors. The first three MAGs had a 130–2359-fold higher abundance in the AW T.15 group, while the latter two MAGs had a 1044–3558-fold higher abundance in the AW T.2 group.

We then compared the distribution of virulence factors present in each MAG depending on the cultivation temperature. For most MAGs, there was a proportional relationship between the log ratio of abundance of MAGs in the AW T.15 group/abundance of MAGs in the AW T.2 group and the log ratio of RPKM of the virulence factors in the AW T.15 group/RPKM of the virulence factors in the AW T.2 group (Fig. 4c). MAGs with a log-ratio greater than 1 for RPKM of the virulence factors, i.e., MAGs with more virulence factors in the AW T.15 group than in the AW T.2 group, belonged to 1G12 (Bin54), *V. splendidus* D (Bin95), and *Pseudomonas E* GCF_0010345.1 (Bin82). On the other hand, MAGs with a log-ratio lesser than 1 for RPKM of the virulence factors belonged to *Arcobacter* (Bin44_0), *Nonlabens* (Bin122), and LS-SOB (Bin23). To determine which virulence factor genes were frequently found in the T.2 and T.15 groups, we confirmed the virulence factors present in six MAGs: three MAGs with the highest log ratio of AW T.15/AW T.2 for RPKM of the virulence factors and three with the lowest (Table 1). A sugar nucleotidyltransferase (*Cj1416c*) was found in all six MAGs. Moreover, a two-component response regulator (*fleR*), the flagellar basal body rod modification protein FlgD (*flgD*), and dTDP-4-dehydrohamnose 3,5-epimerase (*rfbC*) were detected in all three MAGs with the highest log ratio of AW T.15/AW T.2.

Table 1
List of virulence factors found in six MAGs, which accounted for the highest and lowest ratios of RPKM of the virulence factors in the T.15 group/RPKM of virulence factors in the T.2 group.

MAGs	Virulence Factors	AW T.2	AW T.8	AW T.15
1G12 Bin54	(*ascS*) type III secretion system inner membrane export apparatus protein, AscS	2.60	249.02	189.18
	(*Cj1416c*) sugar nucleotidyltransferase	3.24	121.97	195.28
	(*fleR*) two-component response regulator	3.40	240.80	291.25
	(*flgD*) flagellar basal body rod modification protein, FlgD	1.65	136.20	183.25
	(*rfbC*) dTDP-4-dehydrorhamnose 3,5-epimerase	0.49	1584.87	1792.13
Vibrio splendidus D Bin95	(*algQ*) alginate regulatory protein, AlgQ	5.25	17.74	464.84
	(*algU*) alginate biosynthesis protein, AlgZ/FimS	1.10	5.54	378.22
	(*ascS*) type III secretion system inner membrane export apparatus protein, AscS	1.71	26.19	809.20
	(*Cj1416c*) sugar nucleotidyltransferase	5.73	55.61	2710.75
	(*clpP*) ATP-dependent Clp protease proteolytic subunit	0.91	2.15	142.70
	(*fleR*) two-component response regulator	18.36	5.37	251.36
	(*flgD*) flagellar basal body rod modification protein, FlgD	3.35	5.40	175.84
	(*pchB*) salicylate biosynthesis protein, PchB	6.42	74.84	3934.95
	(*rfaD*) ADP-L-glycero-D-mannoheptose-6-epimerase	0.40	5.76	251.30
	(*rfaE*) ADP-heptose synthase	0.13	2.77	148.73
	(*rfbC*) dTDP-4-dehydrorhamnose 3,5-epimerase	2.44	12.08	614.17
	(*ureB*) urease beta subunit UreB, urea amidohydrolase	0.59	3.24	236.72
	(*ureG*) urease accessory protein	0.00	4.02	261.69
	(*virD4*) type IV secretion system component, VirD4	0.89	3.91	123.41
GCF001050345.1 Bin82	(*algA*) phosphomannose isomerase/guanosine 5'-diphospho-D-mannose pyrophosphorylase	0.00	0.06	2.14

MAGs	Virulence Factors	AW T.2	AW T.8	AW T.15
	(*algQ*) alginate regulatory protein, AlgQ	0.00	0.00	5.16
	(*algR*) alginate biosynthesis regulatory protein, AlgR	0.25	0.00	4.92
	(*algU*) alginate biosynthesis protein AlgZ/FimS	0.00	0.00	8.07
	(*bplB*) probable acetyltransferase	0.00	0.00	38.32
	(*Cj1416c*) sugar nucleotidyltransferase	2.37	0.00	11.45
	(*fbpC*) iron(III) ABC transporter ATP-binding protein	1.09	0.00	30.31
	(*fleR*) two-component response regulator	0.28	0.00	8.17
	(*flgD*) flagellar basal body rod modification protein, FlgD	0.21	0.00	3.35
	(*motA*) flagellar motor protein	0.00	0.00	2.20
	(*motA*) flagellar motor protein, MotA	0.00	0.00	2.16
	(*mucA*) alkaline metalloproteinase precursor	0.11	0.00	5.69
	(*mucB*) anti-sigma factor MucA, inhibitor of *alg* expression	0.00	0.00	6.45
	(*pchB*) salicylate biosynthesis protein, PchB	0.07	0.00	4.95
	(*pilC*) still frameshift type 4 fimbrial biogenesis protein, PilC	0.00	0.00	2.94
	(*pvdE*) pyoverdine biosynthesis protein, PvdE	0.00	0.00	3.97
	(*rfbC*) dTDP-4-dehydrorhamnose 3,5-epimerase	0.65	0.10	48.71
	(*ureG*) urease accessory protein	0.31	0.00	2.66
	(*vipB*/*mglB*) type VI secretion system tubule-forming protein, VipB	0.00	0.06	5.42
	(*virD4*) type IV secretion system component, VirD4	0.34	0.00	3.50
	(*waaA*) lipopolysaccharide core biosynthesis protein, WaaP	0.20	0.00	2.30
	(*xcpA*/*pilD*) type 4 prepilin peptidase, PilD	0.00	0.00	3.25
LS-SOB Bin23	(*ascS*) type III secretion system inner membrane export apparatus protein, AscS	21.27	0.00	0.00
	(*Cj1416c*) sugar nucleotidyltransferase	59.33	0.00	0.00

MAGs	Virulence Factors	AW T.2	AW T.8	AW T.15
	(*fleR*) two-component response regulator	29.63	0.03	0.47
	(*flgD*) flagellar basal body rod modification protein, FlgD	17.91	0.00	0.00
Nonlabens Bin122	(*ascS*) type III secretion system inner membrane export apparatus protein, AscS	34.20	0.15	0.18
	(*Cj1416c*) sugar nucleotidyltransferase	42.36	0.00	0.00
	(*fleR*) two-component response regulator	35.96	0.26	0.07
	(*flgD*) flagellar basal body rod modification protein, FlgD	45.72	0.11	0.04
Arcobacter Bin44_0	(*algQ*) alginate regulatory protein, AlgQ	90.41	0.00	0.10
	(*Cj1416c*) sugar nucleotidyltransferase	352.84	0.00	0.18
	(*clpP*) ATP-dependent Clp protease proteolytic subunit	233.41	0.00	0.00

CAZymes and chitinase in MAGs from T. kingsejongensis **stool samples**

To assess CAZymes in MAGs from copepod stool samples, we annotated metagenome data using run-dbcan v2.0.6. We detected a total of 1,991 CAZymes, including 850 glycoside hydrolases (GHs), 763 glycosyltransferases (GTs), 195 carbohydrate esterases (CEs), 89 carbohydrate-binding modules (CBMs), 55 polysaccharide lyases (PLs), and 39 auxiliary activities (AAs), in all 44 MAGs, except for UBA6164 (Bin101). In the 850 GHs, 126 families were identified; the most abundant GHs were identified to be GH23, GH3, and GH20 (Fig. 5a). Most GHs were more frequently found in MAGs in the AW T.15 group than in the AW T.8 and AW T.2 groups.

Then, MAGs were screened for the presence of GHs annotated to chitinase, which bacteria use to mineralize the exoskeleton and fecal pellets of copepods. Three GHs (GH18, GH19, and GH23) encoding chitinase were detected (Fig. 5b). The relative abundance of these GHs increased with increasing cultivation temperature; GH23 was the most abundant GH annotated to chitinase. Moreover, the number of CAZymes increased as the MAG size increased (Fig. 5c). *Polaribacter* (Bin88) contained many CAZymes, while Saprospiraceae (Bin80) and *Aureispira* (Bin107) contained a small number of CAZymes despite their large genome size. Of the 43 MAGs containing CAZymes, 31 MAGs had GHs encoding chitinase in their contigs. Of these, MAGs belonging to *Jiulongibacter* (Bin10), *Maribacter* (Bin28), *Pseudoalteromonas* (Bin136), Cyclobacteriaceae (Bin117), and *V. splendidus* D (Bin95) contained more than two families of GHs encoding chitinase. Interestingly, *V. splendidus* D (Bin95) had the only MAG containing GH19 and having all three families of GHs encoding chitinase.

Discussion

The present study aimed to identify the effects of increased seawater temperature due to climate changes in the changes in Antarctic copepods' stool microbiome and the population reduction of this cold-adapted copepod. Changes in the seawater temperature can affect the abundance of copepods, which are the primary producers and consumers of seawater. In addition, changes in the copepod population can alter the entire seawater ecosystem. There are two explanations of how copepods are affected by temperature increases: (1) changes in the temperature of the host environment directly affect the physiology of copepods and/or (2) increased temperature alters the gut microbiome, which then changes the host physiology and other aspects. In general, the gut microbiome affects the host physiology, growth, immune system, and health. We used this approach to characterize the copepod stool microbiome depending on cultivation temperatures and developmental stages in the present study.

16S rRNA gene sequencing revealed different stool microbial communities at different temperatures and a decreasing alpha diversity pattern with increasing temperature. We identified *Colwellia* as a strict psychrophilic microbe found in cold marine environments, including deep-sea and Antarctic sea ice, primarily observed in *T. kingsejongensis* in the T.2 group [35]. On the other hand, in the *T. kingsejongensis* at 15°C, the genus *Vibrio* was higher than in low temperatures. These results could be explained in two possibilities. One is that a higher temperature is suitable for the fitness of *Vibrio* and its relative abundance increased with increasing temperatures. The second is that there is no control in the microbial community, and a new microbe cannot enter the bacterial pool in the closed experimental condition, the *T. kingsejongensis* gut. Microbes may need to adapt to changes in cold-adapted copepods with temperature changes. Therefore, in bacterial communities that lose their diversity, the population of specific bacteria rapidly increases, eventually leading to the loss of intrinsic functions, such as digestion, nutrient uptake, reproduction, immune response, and other host defenses.

The abundance of copepod populations shows a clear seasonal and horizontal distribution pattern [36, 37]. Copepod species show the highest abundance during spring, and their abundance is low in the warm water environment (> 10–12°C) during later summer and fall in the Gulf of Maine region [38]. Moreover, temperature affects to reproduction and development of some copepod. Different copepod species had distinct temperature ranges for reproduction and development and showed different reproduction patterns in each incubation temperature [39]. The egg production of female calanoid copepod *Pseudodiaptomus annandalei* was significantly lower compared to females at higher temperatures [40]. It is clear that the growth, development, and reproduction of copepods are influenced by water temperature changes [39, 41]. Here, we observed the differences of microbial diversity and the gut microbial community of nauplius and egg-attached at the same temperature, 8°C. These results that change of copepod’s gut microbiome depending on their developmental stage suggested that the gut microbiome indirectly affects the changes in copepod populations.

In the present study, we recovered 44 MAGs from *T. kingsejongensis* stool samples. We found that both Proteobacteria and Bacteroidetes were dominant in the copepod stool microbiome at three different temperatures (2°C, 8°C, and 15°C). Proteobacteria and Bacteroidetes are commonly observed in the intestines of aquatic animals. These two phyla have been found to be distributed in the stools of marine

animals, including *Litopenaeus vannamei* [42], *Penaeus monodon* [43], the mitten crab *Eriocheir sinensis* [44], and the sea lamprey *Petromyzon marinus* [45]. At the genus level, the relative abundance of *Colwellia* and *Arcobacter* lowered, while *Vibrio, Pseudomonas*, and *Pseudoalteromonas* increased with an increase in cultivation temperature. These results are similar to those reported Moisander et al. [46]. They revealed that Proteobacteria and Bacteroidetes were the predominant phyla, and Vibrionaceae and *Pseudoalteromonas* were abundant in copepod stools at 16°C.

Vibrio, belonging to Vibrionaceae, showed higher abundance at higher temperatures. A number of *Vibrio* species have a mechanism to degrade chitin, a component of the copepod surface [17]. We assumed that an increase in the abundance of *Vibrio* species having certain genes, including the gene encoding chitinase, affects copepod development at higher temperatures. Through CAZyome annotation, we identified GHs encoding chitinase, including GH18, GH19, and GH23, were more abundant at higher temperatures. These GHs were mainly found in the MAG of *V. splendidus* D, and this MAG was abundant at 15°C. More chitinase is found at a higher temperature than at a lower temperature, implying that higher temperature is more suitable for bacteria to mineralize the exoskeleton and fecal pellets of copepods. In addition, MAG annotation using VFDB revealed the virulence factors present at a higher temperature (15°C). Virulence factors can be divided into three groups according to their function. We revealed that virulence factors belonging to all three groups were present in MAGs from *T. kingsejongensis* [47]: membrane proteins playing a role in adhesion, colonization, and invasion (*pchB*, *flgD*, *ureG*, *algQ*, and *algU*); polysaccharide capsules for surrounding the bacterial cell (*rfbC*); and secretory proteins (*ascS* and *virD4*). An increase in virulence factors suggests that specific *Vibrio* strains are likely to affect copepod development directly. The gene *pchB* (encoding salicylate biosynthesis protein) and *ureG* and *ureB* (encoding urease-related protein) have been studied with regard to antibiotic resistance or the colonization of bacteria [48, 49], whereas *rfbC* (encoding dTDP-4-dehydrorhamnose 3,5-epimerase) is known for increasing bacterial adherence and immune invasion [50].

As the current temperature of Antarctic seawater has not increased to 8°C or 15°C, it is not possible to know the effects in the real environment. However, this study emphasizes the need to prepare for climate change based on the experimental results that an increasing temperature affects the population and growth of cold-adapted copepods and their stool microbiome. In the present study, we confirmed a lower microbial diversity and a lower number of egg-attached copepods at a higher temperature, 15°C. Therefore, failure to regulate the growth of copepods with an increase in temperature will affect the population of copepods, which play an essential role in the seawater ecosystem, thereby disrupting the seawater ecosystem as a whole.

Declarations

FUNDING

This research was supported by the Chung-Ang University Graduate Research Scholarship in 2016. This work was supported by the National Research Foundation of Korea(NRF) grant funded by the Korea

government(MSIT) (NRF-2019R1A2C1090861) and a research grant(PE21140) by the Korea Polar Research Institute.

CONFLICTS OF INTEREST

The authors have no conflicts of interest to declare.

AVAILABILITY OF DATA AND MATERIAL

16S rRNA gene sequence data from the present study have been archived at the NCBI Sequence Read Archive (SRA) under the accession number SRR12538744-12538756 and BioProject accession number PRJNA659815 and shotgun metagenome sequence data is available at SRA under the accession number SRR12549471-12549473 and BioProject accession number PRJNA660278.

AUTHORS' CONTRIBUTIONS

WJS and SK designed the research study; HNO, G-SK, TK, and MNR conducted the research; HNO, TK, and WJS analyzed the data; TK and HNO prepared all the figures; and HNO and WJS wrote the main manuscript.

References

1. Lopes RM, Reid JW, Rocha CE (2001) Copepoda: Developments in Ecology, Biology and Systematics: proceedings of the Seventh international conference on Copepoda, held in Curitiba, Brazil, 25–31 July, 1999: reprinted from Hydrobiologia, vol. 453/454 (2001). Springer Science & Business Media
2. Sieburth JM, Smetacek V, Lenz J (1978) Pelagic ecosystem structure: Heterotrophic compartments of the plankton and their relationship to plankton size fractions 1. Limnol Oceanogr 23:1256–1263
3. Calbet A (2008) The trophic roles of microzooplankton in marine systems. ICES J Mar Sci 65:325–331
4. GIFFORD DJ (1991) The protozoan-metazoan trophic link in pelagic ecosystems. The Journal of protozoology 38:81–86
5. Calbet A, Saiz E (2005) The ciliate-copepod link in marine ecosystems. Aquat Microb Ecol 38:157–167
6. Turner JTJZs (2004) The importance of small planktonic copepods and their roles in pelagic marine food webs43: 255–266
7. Sochard M, Wilson D, Austin B, Colwell R (1979) Bacteria associated with the surface and gut of marine copepods. Appl Environ Microbiol 37:750–759
8. Carman KR, Dobbs FC (1997) Epibiotic microorganisms on copepods and other marine crustaceans. Microscopy research technique 37:116–135
9. Harris JM (1993) The presence, nature, and role of gut microflora in aquatic invertebrates: a synthesis. Microbial ecology 25:195–231

10. Nagasawa S, Nemoto T (1988) Presence of bacteria in guts of marine crustaceans and on their fecal pellets. J Plankton Res 10:559–564
11. Gerdts G, Brandt P, Kreisel K, Boersma M, Schoo K, Wichels A (2013) The microbiome of North Sea copepods. Helgol Mar Res 67:757–773
12. Yeh HD, Questel JM, Maas KR, Bucklin A (2020) Metabarcoding analysis of regional variation in gut contents of the copepod Calanus finmarchicus in the North Atlantic Ocean. Topical Studies in Oceanography, Deep Sea Research Part, p 104738
13. Rivera G, Souza IN, KMCd S, CPd, Lopes RM (2013) Free-living and plankton-associated vibrios: assessment in ballast water, harbor areas, and coastal ecosystems in Brazil. Frontiers in microbiology 3:443
14. Møller EF, Nielsen TG (2001) Production of bacterial substrate by marine copepods: effect of phytoplankton biomass and cell size. J Plankton Res 23:527–536
15. Pruzzo C, Vezzulli L, Colwell RR (2008) Global impact of Vibrio cholerae interactions with chitin. Environ Microbiol 10:1400–1410
16. Paulsen SS, Andersen B, Gram L, Machado H (2016) Biological potential of chitinolytic marine bacteria. Marine drugs 14:230
17. Mondal M, Nag D, Koley H, Saha DR, Chatterjee NS (2014) The Vibrio cholerae extracellular chitinase ChiA2 is important for survival and pathogenesis in the host intestine. PLoS One 9:e103119
18. Homonnay ZG, Kéki Z, Márialigeti K, Tóth EM (2012) Bacterial communities in the gut of the freshwater copepod Eudiaptomus gracilis. J Basic Microbiol 52:86–90
19. Møller EF, Riemann L, Søndergaard M (2007) Bacteria associated with copepods: abundance, activity and community composition. Aquat Microb Ecol 47:99–106
20. Park E-O, Lee S, Cho M, Yoon SH, Lee Y, Lee W (2014) A new species of the genus Tigriopus (Copepoda: Harpacticoida: Harpacticidae) from Antarctica. Proceedings of the Biological Society of Washington 127: 138–154
21. Kim B-M, Jeong C-B, Lee MC, Rhee J-S, Lee J-S (2015) Identification of the retinoblastoma (Rb) gene and expression in response to environmental stressors in the intertidal copepod Tigriopus japonicus. Mar Genom 24:387–396
22. Eren AM, Vineis JH, Morrison HG, Sogin ML (2013) A filtering method to generate high quality short reads using Illumina paired-end technology. PloS one 8:e66643
23. Caporaso JG, Kuczynski J, Stombaugh J, Bittinger K, Bushman FD, Costello EK, Fierer N, Pena AG, Goodrich JK, Gordon JI (2010) QIIME allows analysis of high-throughput community sequencing data. Nature methods 7:335–336
24. Edgar RC (2010) Search and clustering orders of magnitude faster than BLAST. Bioinformatics 26:2460–2461
25. Quast C, Pruesse E, Yilmaz P, Gerken J, Schweer T, Yarza P, Peplies J, Glöckner FO (2012) The SILVA ribosomal RNA gene database project: improved data processing and web-based tools. Nucleic acids

research 41:D590–D596

26. Wang Q, Garrity GM, Tiedje JM, Cole JR (2007) Naive Bayesian classifier for rapid assignment of rRNA sequences into the new bacterial taxonomy. Appl Environ Microbiol 73:5261–5267
27. Li P-E, Lo C-C, Anderson JJ, Davenport KW, Bishop-Lilly KA, Xu Y, Ahmed S, Feng S, Mokashi VP, Chain PS (2017) Enabling the democratization of the genomics revolution with a fully integrated web-based bioinformatics platform. Nucleic acids research 45:67–80
28. Xu H, Luo X, Qian J, Pang X, Song J, Qian G, Chen J, Chen S (2012) FastUniq: a fast de novo duplicates removal tool for paired short reads. PloS one 7:e52249
29. Li D, Luo R, Liu C-M, Leung C-M, Ting H-F, Sadakane K, Yamashita H, Lam T-W (2016) MEGAHIT v1. 0: A fast and scalable metagenome assembler driven by advanced methodologies and community practices. Methods 102:3–11
30. Alneberg J, Bjarnason BS, De Bruijn I, Schirmer M, Quick J, Ijaz UZ, Lahti L, Loman NJ, Andersson AF, Quince C (2014) Binning metagenomic contigs by coverage and composition. Nature methods 11:1144–1146
31. Li H (2013) Aligning sequence reads, clone sequences and assembly contigs with BWA-MEM. arXiv preprint arXiv:13033997
32. Chaumeil P-A, Mussig AJ, Hugenholtz P, Parks DH (2020) GTDB-Tk: a toolkit to classify genomes with the Genome Taxonomy Database. Oxford University Press
33. Zhang H, Yohe T, Huang L, Entwistle S, Wu P, Yang Z, Busk PK, Xu Y, Yin Y (2018) dbCAN2: a meta server for automated carbohydrate-active enzyme annotation. Nucleic Acids Res 46:W95–W101
34. Chen L, Zheng D, Liu B, Yang J, Jin Q (2016) VFDB 2016: hierarchical and refined dataset for big data analysis—10 years on. Nucleic acids research 44: D694–D697
35. Methé BA, Nelson KE, Deming JW, Momen B, Melamud E, Zhang X, Moult J, Madupu R, Nelson WC, Dodson RJJPotNAoS (2005) The psychrophilic lifestyle as revealed by the genome sequence of Colwellia psychrerythraea 34H through genomic and proteomic analyses102: 10913–10918
36. Beaugrand G, Reid PC, Ibanez F, Lindley JA, Edwards M (2002) Reorganization of North Atlantic marine copepod biodiversity and climate. Science 296:1692–1694
37. Hwang J-S, Kumar R, Dahms H-U, Tseng L-C, Chen Q-C (2010) Interannual, seasonal, and diurnal variations in vertical and horizontal distribution patterns of 6 Oithona spp.(Copepoda: Cyclopoida) in the South China Sea. Zoological Studies 49:220–229
38. Ji R, Davis CS, Chen C, Beardsley RC (2009) Life history traits and spatiotemporal distributional patterns of copepod populations in the Gulf of Maine-Georges Bank region. Mar Ecol Prog Ser 384:187–205
39. Halsband-Lenk C, Hirche H-J, Carlotti F (2002) Temperature impact on reproduction and development of congener copepod populations. J Exp Mar Biol Ecol 271:121–153
40. Golez MN, Takahashi T, Ishimarul T, Ohno AJPB, Ecology (2004) Post-embryonic development and reproduction of Pseudodiaptomus annandalei(Copepoda: Calanoida)51: 15–25

41. Beaugrand G, Brander KM, Lindley JA, Souissi S, Reid PC (2003) Plankton effect on cod recruitment in the North Sea. Nature 426:661–664
42. Huang Z, Li X, Wang L, Shao Z (2016) Changes in the intestinal bacterial community during the growth of white shrimp, L itopenaeus vannamei. Aquac Res 47:1737–1746
43. Rungrassamee W, Klanchui A, Chaiyapechara S, Maibunkaew S, Tangphatsornruang S, Jiravanichpaisal P, Karoonuthaisiri N (2013) Bacterial population in intestines of the black tiger shrimp (Penaeus monodon) under different growth stages. PloS one 8:e60802
44. Li K, Guan W, Wei G, Liu B, Xu J, Zhao L, Zhang Y (2007) Phylogenetic analysis of intestinal bacteria in the Chinese mitten crab (Eriocheir sinensis). J Appl Microbiol 103:675–682
45. Tetlock A, Yost CK, Stavrinides J, Manzon RG (2012) Changes in the gut microbiome of the sea lamprey during metamorphosis. Appl Environ Microbiol 78:7638–7644
46. Moisander PH, Sexton AD, Daley MC (2015) Stable associations masked by temporal variability in the marine copepod microbiome. PLoS one 10:e0138967
47. Wu H-J, Wang AH, Jennings MP (2008) Discovery of virulence factors of pathogenic bacteria. Curr Opin Chem Biol 12:93–101
48. Serino L, Reimmann C, Baur H, Beyeler M, Visca P, Haas D (1995) Structural genes for salicylate biosynthesis from chorismate in Pseudomonas aeruginosa. Molecular General Genetics MGG 249:217–228
49. Chuang MH, Wu MS, Lin JT, Chiou SH (2005) Proteomic analysis of proteins expressed by Helicobacter pylori under oxidative stress. Proteomics 5:3895–3901
50. Shornikov A, Tran H, Macias J, Halavaty AS, Minasov G, Anderson WF, Kuhn ML (2017) Structure of the Bacillus anthracis dTDP-l-rhamnose-biosynthetic enzyme dTDP-4-dehydrorhamnose 3, 5-epimerase (RfbC). Acta Crystallographica Section F: Structural Biology Communications 73:664–671

Figures

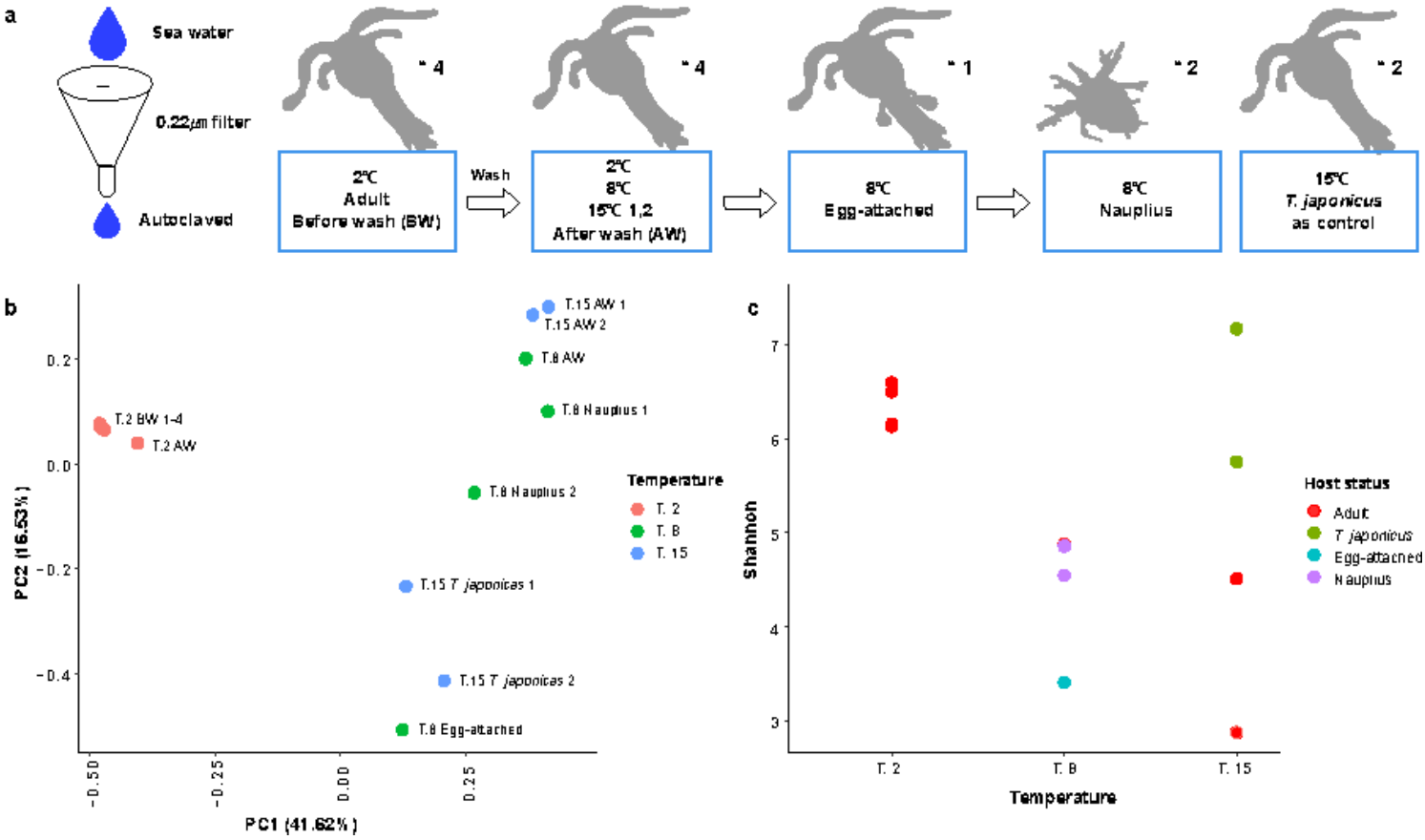

Figure 1

Sample collection method and characteristics of the copepod microbiome. a Sample information used in the present study. b Principal coordinate analysis was performed on the basis of Bray–Curtis distance matrices. c Alpha diversity of the stool microbiome of copepods using the Shannon diversity index.

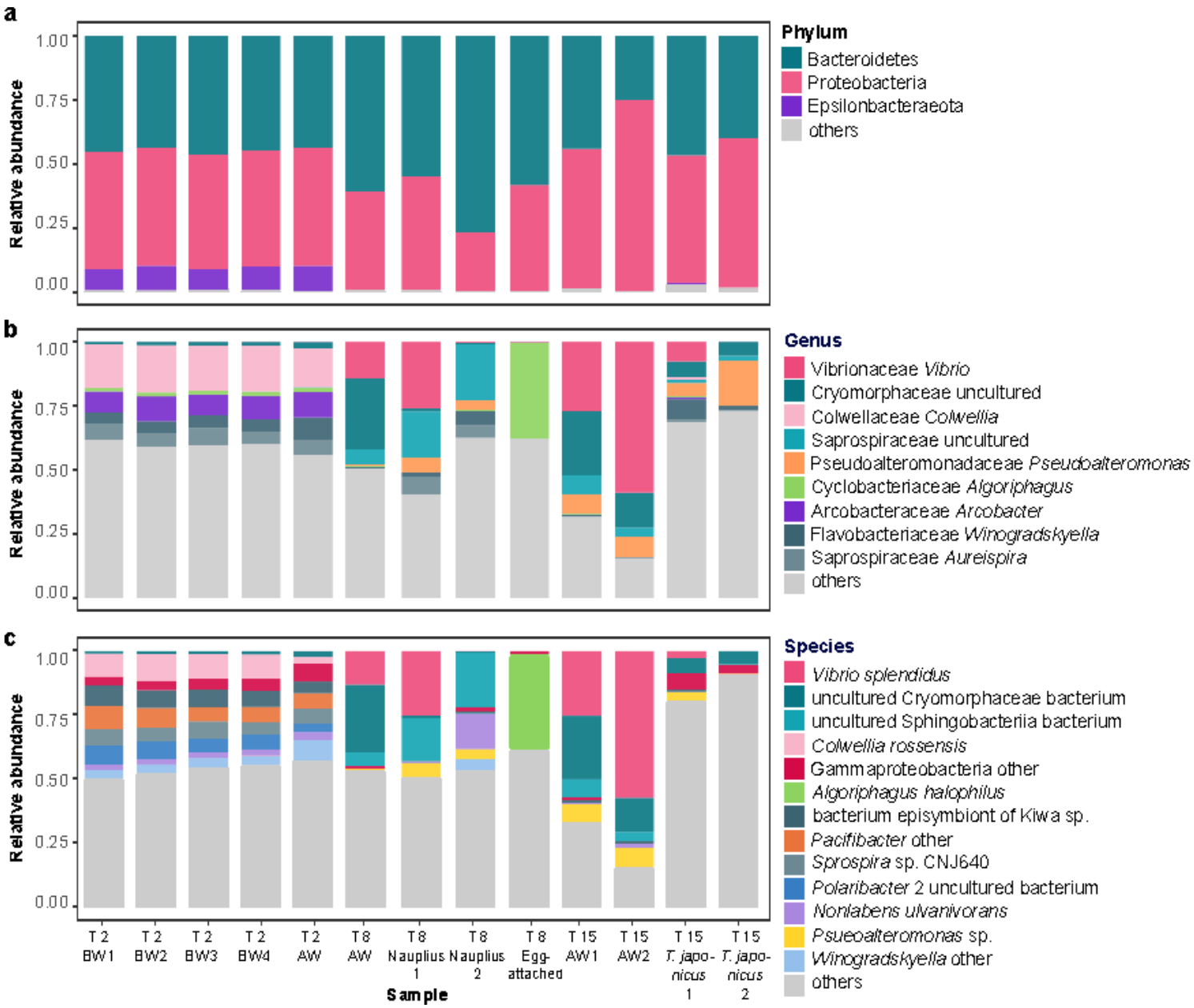

Figure 2

Bar graph of the copepod stool microbiome at the phylum level (a), genus level (b), and species level (c). The X-axis represents each sample, and the y-axis represents the relative abundance of bacteria.

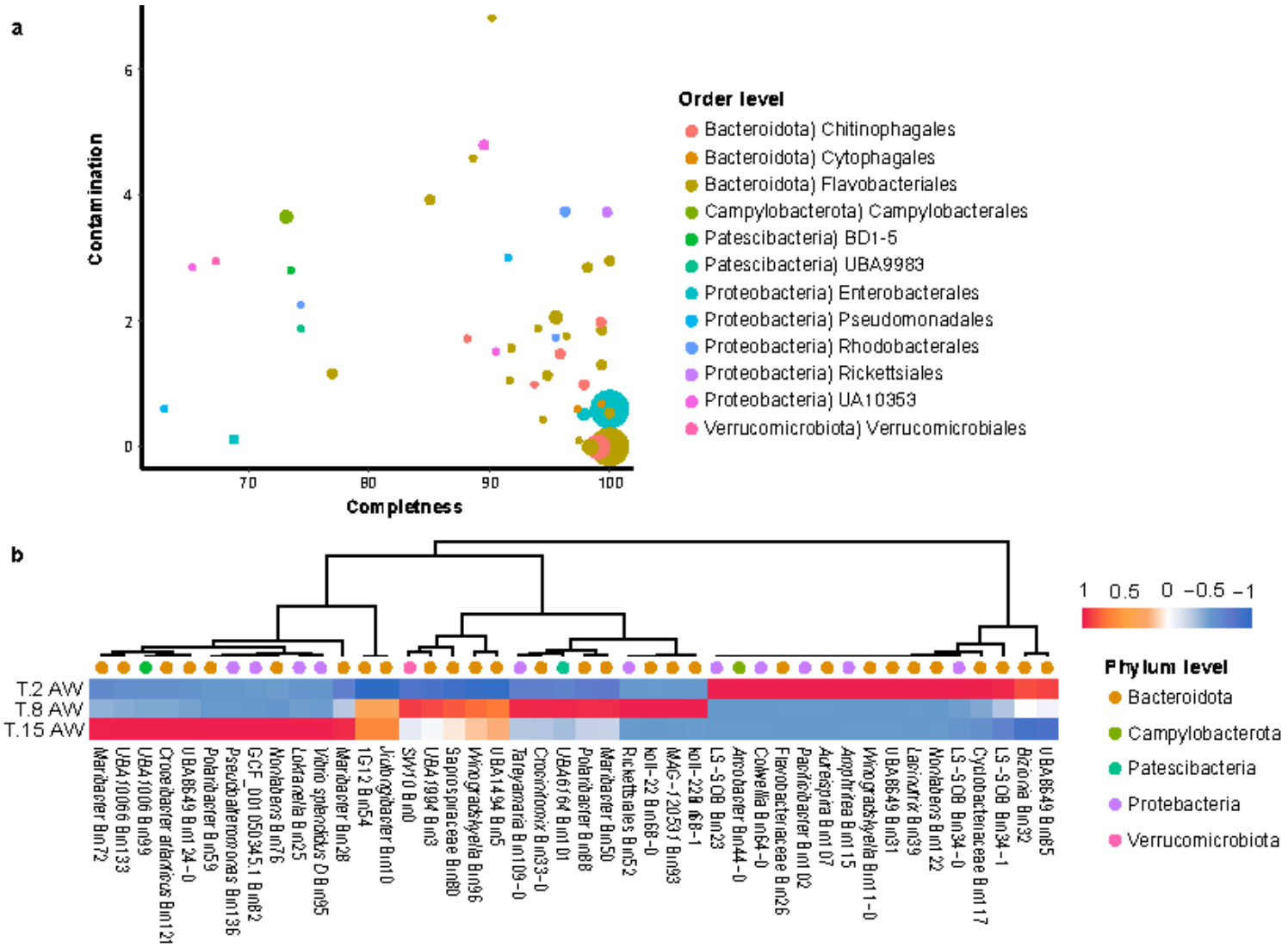

Figure 3

Quality characteristic and relative abundance of 44 reconstructed metagenome-assembled genomes (MAGs). a Completeness and contamination values estimated by CheckM are reported for 44 MAGs. Thirty-four MAGs were high-quality MAGs qualitatively filtered with the criterion of MAG quality score (calculated as completeness − 5 × redundancy) > 50, and 10 MAGs were obtained after pruning. The bubble represents one MAG taxonomically assigned to the order level using the GTDB database, and the size of the bubble is based on the relative abundance. b Heat map for the relative abundance of MAGs of T. kingsejongensis at different cultivation temperatures. The color of the circle above the heat map represents a MAG assigned to the phylum level.

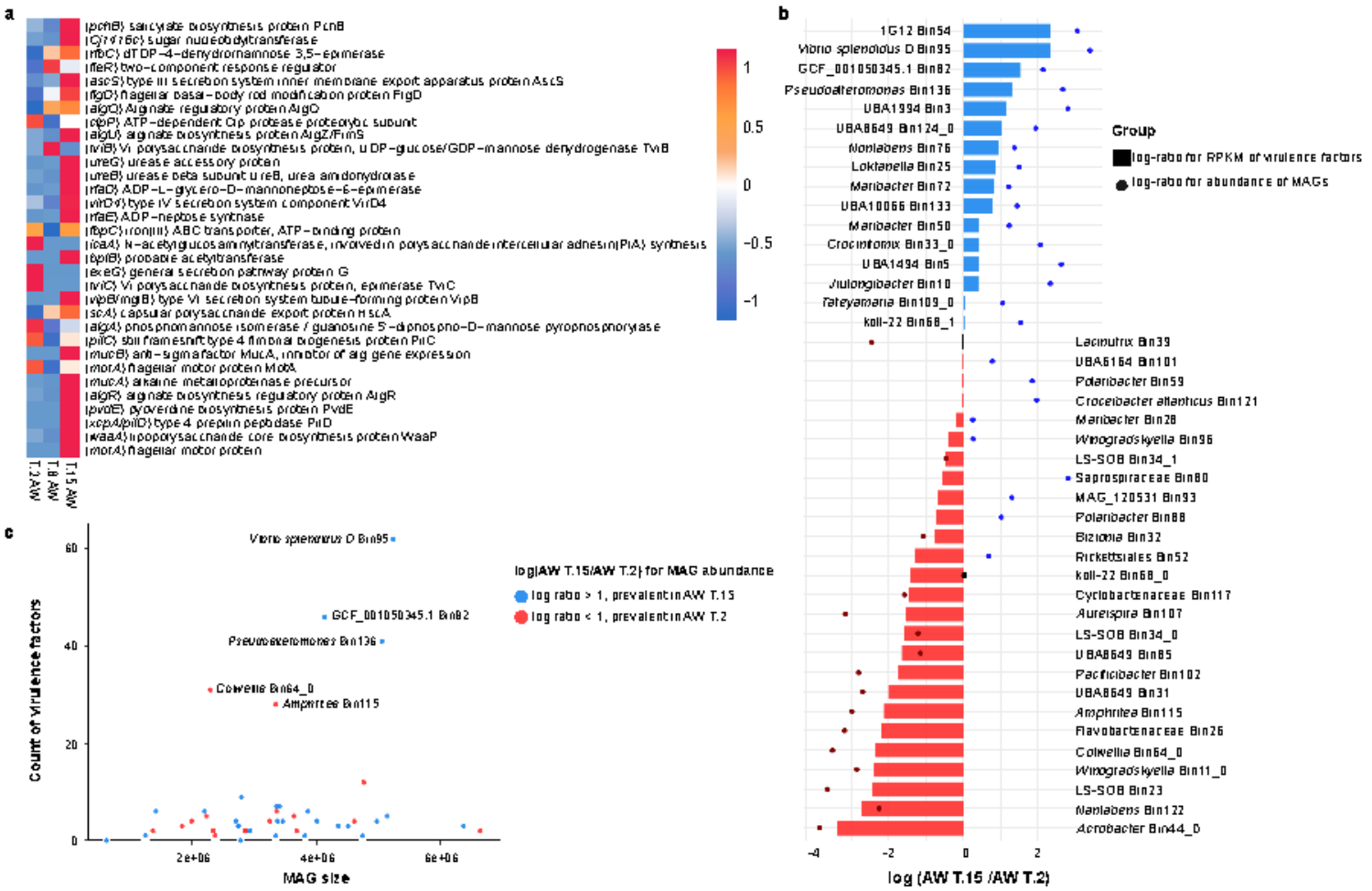

Figure 4

Virulence factors found in MAGs of T. kingsejongensis. a Heat map showing the relative abundance of all virulence factors found in MAGs at each temperature. The relative abundance of virulence factors was calculated as reads per kilobase per million mapped reads (RPKM). b Bar graph of the virulence factors found in each MAG. Each bar represents the value obtained by taking a log of the ratio of RPKM of the virulence factors in the AW T.15 group/RPKM of the virulence factors in the AW T.2 group. Each circle represents the log ratio of the relative abundance of the MAG in the AW T.15 group/relative abundance of the MAG in the AW T.2 group. c Comparison between the size of the MAG and the count of virulence factors found in the MAG. b-c The color of the bar or circle is blue when the log ratio is greater than 1 and red when it is lesser than 1.

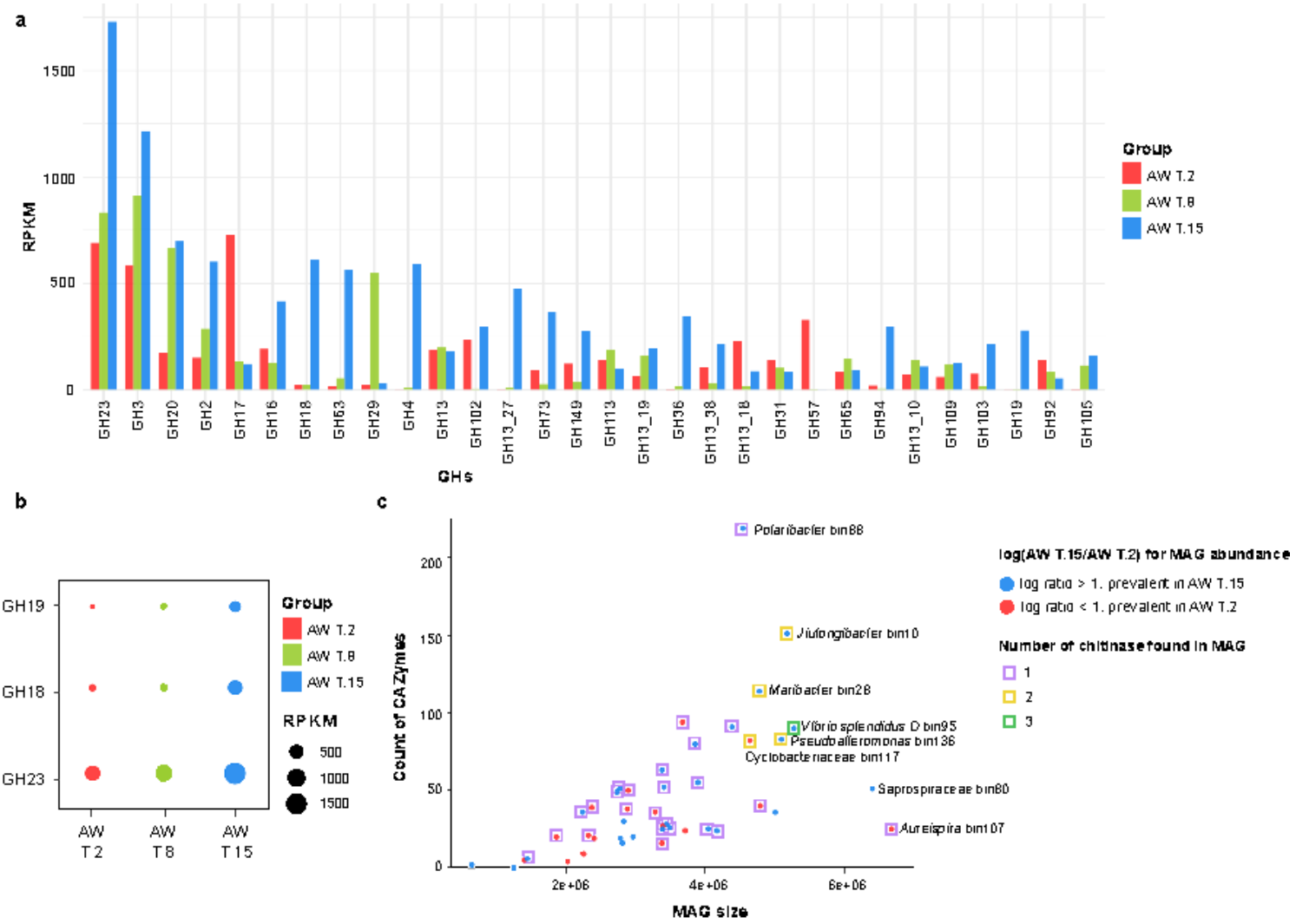

Figure 5

Glycosyl hydrolases (GHs) detected in MAGs. a Bar graph of the 30 most abundant GH families found at three different cultivation temperatures. b Bubble plot of GHs annotated to chitinase identified in MAGs. The size of the bubble is RPKM of chitinase. c Comparison between the size of the MAG and the count of carbohydrate-active enzymes (CAZymes). Each circle represents the log ratio of RPKM of CAZymes in the AW T.15 group/RPKM of CAZymes in the AW T.2 group for an MAG containing CAZymes; CAZymes were identified in 43 out of 44 MAGs. The color of the circle is blue when the log ratio is greater than 1 and red when it is lesser than 1. The rectangular box represents chitinase containing MAG, and the color of the box differs depending on the number of chitinases in the MAG.